A Review of Algorithms and Hardware Implementations in Electrical Impedance Tomography

Zheng Zong, Yusong Wang, and Zhun Wei*

(*Invited*)

Abstract—In recent years, electrical impedance tomography (EIT) has attracted intensive interests due to its noninvasive, ionizing radiation-free, and low-cost advantages, which is promising for both biomedical imaging and industry nondestructive tests. The purpose of this paper is to review state-of-the-art methods including both algorithms and hardware implementations in EIT. More specifically, for the advanced reconstruction algorithms in mainstream, we offer some insights on classification and comparison. As for the measurement equipment, the structure, configuration modes, and typical systems are reviewed. Furthermore, we discuss the limitations and challenges in EIT technique, such as low-spatial resolution and nonlinear-inversion problems, where future directions, such as solving EIT problems with deep learning, have also been addressed.

1. INTRODUCTION

Since electrical impedance tomography (EIT) was proposed, far-reaching developments have taken place in EIT system from algorithm optimizations to hardware designs. Compared with other tomography technologies [1], such as computed tomography (CT), gamma ray tomography, X-ray tomography, ultrasonic imaging, and magnetic resonance imaging (MRI), EIT is a real-time, noninvasive, low-cost, and portable technology which can reflect the internal structures and functions of tissues and organs [2]. Furthermore, it has shown the ability of long-term monitoring of diseases in clinical practice, such as lung function imaging [3, 4], cerebral hemorrhage [5], early detection of breast cancer [6, 7], and gastric emptying detection [8]. Especially during the novel coronavirus (COVID-19), Tomasino and others used EIT technology to evaluate the distribution of ventilation in the different pulmonary regions before, during, and after pronation in COVID-19 respiratory failure in real time [9]. In addition, EIT technology has been under intensive investigations in the fields of industrial process [10], chemical engineering [11], semiconductor manufacturing [12], biotechnology [13, 14], materials [15, 16], artificial sensitive skin [17], hand gesture recognition [18], etc.

Nevertheless, EIT problem, regarded as an inverse problem to restore the unknown impedance of the domain of interest (DOI), is challenging due to its nonlinear and highly ill-posed properties [19–27]. Furthermore, EIT suffers from low spatial resolution, which means that it is challenging for EIT to image an anatomic structure like CT or MRI. A workable proposal is to combine the advantages of EIT and other tomography technologies with high spatial resolution to preserve the morphological structures of the objects and avoid blurring of the solution. For example, Schullcke et al. presented an approach based on discrete cosine transformation (DCT) for EIT image reconstruction, using morphologic information obtained from CT [3]. The results showed that the CT-EIT method improved the accuracy of reconstruction images. Other methods focus on the challenges of mathematical principle

behind the EIT problem to find the approximate solution which is as close to the real solution as possible by optimization modelings and algorithms. In recent decades, a large number of researchers have focused on it where a surging number of state-of-art reconstruction algorithms have been proposed along with the improvements of hardware from generation to generation.

In this paper, we present a review focusing on the reconstruction algorithms and the designs of existing measurement systems in EIT. The text is structured as follows. Section 2 describes the EIT problem with forward problem and inverse problem: the basic concepts of definition and solver. In Section 3, we classify the reconstruction algorithms and review some algorithms proposed in recent years. Section 4 presents the necessary components designed in EIT hardware system and reviews some systems already used in production, living or laboratory. Some conclusions are drawn in Section 5.

2. EIT PROBLEM

A typical schematic of EIT problem is shown in Fig. 1. In the figure, Ω is the area that requires tomography. A total number of N_r electrodes are stuck on the boundary $\partial\Omega$, playing the role of conducting the excitation current j and measuring the boundary voltage $\overline{V}_n$ ($n = 1, 2, ..., N_r$). The edge of domain of interest (DOI) is marked by the dashed line, where the interested electrical impedance σ to be reconstructed is located [20].
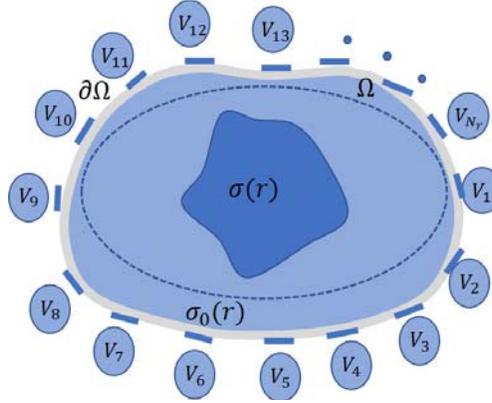
Figure 1. A typical schematic of EIT problem with two dimensional region.

In a certain excitation-measurement mode, the boundary voltages of the body are sampled by EIT hardware system, and then processed in EIT software system to output impedance information of interest. In order to obtain a better understanding of the principle behind this diagram, the concepts of forward and inverse problem are proposed in the rest of the section.

It is noted that electrical impedance can also be expressed by complex admittance γ [26, 27] as

$$\gamma = \sigma + i\omega\epsilon \tag{1}$$

where ω is the angular frequency, σ the electrical conductivity, and ϵ the electric permittivity. Theoretically, EIT is a combination of electrical conductivity tomography (ECT) and electrical permittivity tomography (EPT). However, in many areas applying EIT (i.e., lung imaging), the real part or the static state ($\omega = 0$) of the admittance is more important than others due to additional pathological information [28]. In order to simplify the problem, only the real part needs to be reconstructed. Therefore, in a lot of literatures, the electrical impedance is simplified as electrical conductivity. We also use this simplification in this paper to describe problems more easily.

2.1. Forward Problem

● **Definition.** Calculate the boundary voltage $\overline{V}$ at the measurement electrodes, when the the spatial distribution of conductivity $\sigma(r)$ of the objects and boundary conditions are known.

- **Analysis.** The problem is equal to finding a unique solution of Laplace equation under Newman boundary condition. Specially, based on *Maxwell equation, Ohm law, and charge conservation*, a Laplace equation can be obtained as:

$$\nabla \cdot [\sigma(r)\nabla\varphi(r)] = 0, \ \ r \in \Omega \tag{2}$$

where φ is the electric potential, and Ω is the domain of interest. The boundary condition on electrodes is

$$\sigma(r)\frac{\partial\varphi(r)}{\partial n} = j, \ \ r \in \partial\Omega \tag{3}$$

where j is the current density at the electrodes, and $\partial\Omega$ is the the boundary of the body Ω. In addition, the current conservation equation $\int_{\partial\Omega} j = 0$ needs to be satisfied from Gauss theorem, and zero potential needs to be defined [20, 29, 30]. Due to the irregular boundary shape $\partial\Omega$, it is difficult to get an analytical solution to the above differential equation. Actually, the relationship among excitation, system reaction, and measurement can be represented easily as

$$\overline{V} = \mathbf{F}(\sigma(r))|_j \tag{4}$$

where $\sigma(r)$ is the conductivity distribution; $\overline{V}$ represents the theoretical boundary voltage; $\mathbf{F}$ is a nonlinear function mapping from the conductivity distribution space to measurement space.
- **Solver.** Based on the modeling of electrodes, EIT solver can be classified into continuum model, gap model, shunt model, and complete model [29, 31]. Regardless of the models used, $\mathbf{F}$ is always a nonlinear function which is hard to express analytically. For this reason, some methods use Taylor's formula for linearization approximation [32–35], such as

$$\overline{V} = \overline{V}_0 + \Delta\overline{V} \approx \mathbf{F}(\sigma_0)|_j + \frac{\partial\mathbf{F}(\sigma)|_j}{\partial\sigma}|_{\sigma_0} \cdot \Delta\sigma = \mathbf{F}(\sigma_0)|_j + \overline{\overline{\mathbf{J}}} \cdot (\sigma(r) - \sigma_0) \tag{5}$$

where σ_0 is the background materials referred to as inclusions, the sensitivity matrix $\overline{\overline{\mathbf{J}}}$, also frequently referred to as the Jacobian matrix, and maps the conductivity distribution to measurement distribution. When the electrode positions and current injection/measurement protocol are determined, $\overline{\overline{\mathbf{J}}}$ can be computed with the finite element method (FEM) [32]. In addition to the above linear approximation solver, another typical solver of the nonlinear function $\mathbf{F}$ is as follows [20, 36, 37], given through Green's Theorem and Method of Moments (MOM):

$$Current \ State \ Equation: \ \overline{J} = \overline{\overline{\xi}} \cdot \left(\overline{E^i} + \overline{\overline{G}}_D \cdot \overline{J}\right) \tag{6}$$

$$Voltage \ Data \ Equation: \ \overline{V} = \overline{\overline{G}}_S \cdot \overline{J} \tag{7}$$

where $\overline{\overline{\xi}}$ is defined as the contrast inclusion to represent $\sigma(r) - \sigma_0$; $\overline{E^i}$ is the electric field when there is no inclusion presented in the domain Ω; $\overline{\overline{G}}_D$ and $\overline{\overline{G}}_S$ are the linear transformation from induced contrast current $\overline{J}$ space to induced contrast electric field space in Ω and scattering voltage space at $\partial\Omega$, respectively, both of which can be computed with numerical software.

2.2. Inverse Problem

- **Definition.** Find the the spatial distribution of conductivity $\sigma(r)$ of the objects if the boundary conditions and the voltage $\overline{V}_n$ at the measurement points are known.
- **Analysis.** From the perspective of Eq. (4), the inverse problem can be expressed as

$$\sigma(r) = \mathbf{F}^{-1}(\overline{V}_n)|_j \tag{8}$$

where $\overline{V}_n$ is the measurement boundary voltage with noise different from the forward problem solver $\overline{V}$. According to Eq. (8), two major challenges are proposed.

Firstly, the mapping $\mathbf{F}$ is nonlinear, and it is difficult to find the inverse mapping $\mathbf{F}^{-1}$ analytically.

Secondly, the theoretical boundary voltage $\overline{V}$ regarded as the forward problem solver satisfies an elliptic equation with Cauchy data [26], which means that the problem is ill-posed, and a small perturbation (i.e., noise) in the measurement data $\overline{V}_n$ will have a great impact on the solution $\sigma(r)$.
- **Solver.** In recent years, a large number of scholars focus on inverse solver of EIT, and a lot of state-of-art algorithms have been proposed. In the next section, we will review typical inverse solvers.

3. ALGORITHM IMPLEMENTS

In the past decades, the EIT topic has been reviewed in some literatures [19, 26, 27, 38–40]. With the development of both algorithms and hardware implementations, intensive progresses have been achieved in EIT technique. For example, the learning algorithm becomes more and more attractive in the inverse problem, where stunning success has been shown in reconstructed image quality, robustness, and speed of solving EIT problems [20, 36, 41–46]. In this section, we will review and classify some classical reconstruction algorithms and discuss possible improved methods.

3.1. Model-Based Approach

To date, two major models of EIT problem exist in model-based approach, pixel/voxel-based image reconstruction and shape-based image reconstruction. The former is essentially the estimation of the unknown conductivity distribution, while the latter is geometrical representation of scatters [47]. For both kinds of modeling methods, expressing the inverse map $\mathbf{F}^{-1}(\overline{V}_n)$ is laborious and even impossible, thus an optimization criterion is typically chosen [38] such as minimizing a $l2$ norm loss functions, minimizing a variational function, and maximum posteriori, usually derived from the forward problem. Once a reasonable criterion is established, the remaining work is just to find a suitable algorithm to solve the equation. The iterative algorithms are very suitable for solving the nonlinear inverse problem, such as some Newton-type algorithms [23, 47], nonlinear conjugate gradient algorithms [20], and ADMM optimization algorithm [48]. In addition, some non-iterative algorithms are also used to solve the model of inverse problem, such as D-bar method [49] and factorization method [50]. It is noted that no matter what kind of algorithm is used, the convergence of the objective function and the uniqueness of the regularized solution should be warranted [26, 48].

According to whether the unknown σ is regarded as a random variable, we divide the model-based approach into the deterministic method and stochastic method.

• **Deterministic method**

In this method, the unknown σ is regarded as the deterministic result of the electrodynamics principle. Some classes of optimization criterion are proposed to obtain the unknown σ [26, 70]:

One is called *Output Least squares* methods, and the idea is to minimize the function of some $l2$ norm with a regularizer that imposes a prior information into the solution, such as

$$\widehat{\sigma}(r) = \arg\min_{\sigma} \sum_{e=1}^{N} \left\| F(\sigma(r)) - \overline{V}_{n,e} \right\|^2 + R(\sigma(r)) \tag{9}$$

where $l2$ norm term is the appellation of data-fidelity that penalizes the mismatch between the forward solver $\overline{V}$ and the measurement value $\overline{V}_n$, and $R(\sigma)$ is the regularizer that incorporates a prior knowledge into the objective function. Some kinds of regularization term have been applied in EIT, such as smoothing $l2$ norm regularization [51], total variation (TV) regularization that preserves the edges [20, 52], sparsity regularization (SR) with sharp boundaries [53], and multiplicative regularization (MR) which does not require to set an artificial parameter [23], where the regularization term always plays a crucial role in the deterministic method. It is noted that there are several optimization criteria using the *Output Least Square* method more than the form in Eq. (9), such as ROI constrained linear difference reconstruction and nonlinear difference imaging approach [21].

Besides the *Output Least squares* methods, the *Variational* method, derived from variational principles [54], is also regarded as an popular optimization criterion for deterministic method. This algorithm reconstructs σ by minimizing

$$\widehat{\sigma} = \arg\min_{\sigma} \sum_{e=1}^{N} \int_{\Omega} \left| \sigma^{\frac{1}{2}}(r)\nabla\overline{V}_{n,e} + \sigma^{-\frac{1}{2}}(r)j_e \right|^2 \mathrm{d}r \tag{10}$$

where $V_{n,e}(x)$ and j_e are the e-th measurement and excitation value at $\partial\Omega$.

In addition, an original optimization criterion called *level set* methods has been applied in EIT algorithms recently, where numerous techniques such as shape derivatives and topological derivatives have been included in it to analyse problems referring to shape optimization [70, 71].

- **Stochastic method**

In this method, all unknowns are regarded as random quantities which follow the maximum likelihood method, maximum a posteriori method or Bayesian method [38]. For example, optimization in Eq. (9) is interpreted in a Bayes perspective to maximize the posterior [32]:

$$\arg\max_{\sigma} p\left(\sigma \mid \overline{V}_n\right) \triangleq \arg\min_{\sigma} \left[-\log p\left(\overline{V}_n \mid \sigma\right) - \lambda \log p(\sigma)\right] \tag{11}$$

where the prior knowledge is clearly introduced into the formula with a specific probability $p(\sigma)$ (for example, Gaussian or Dirichlet distribution or flat distribution), and the probability $p(\overline{V}_n \mid \sigma)$ is generated from the forward solver with $\overline{V}_n = \overline{V} + \overline{n}$, in which $\overline{n}$ is the Gaussian noise vector. Eq. (11) is used to give a description of the probabilistic distribution instead of deterministic values of the unknown σ.

Deterministic method contains a clearer physical meaning, while stochastic method allows to quantify the uncertainty in restoration and the statistical properties of data and noise. To contextualize a clearer framework among model-based approaches, Table 1 summarizes the algorithms in the last three years.

Table 1. A summary of algorithms applied in EIT in the last three years.

	Name	Model	Dimension	Optimization criterion	Optimization method	Regularization	Innovation
Deterministic method	Bases-Expansion Subspace Optimization Method (BE-SOM) [20]	Pixel/voxel-based	2D	Least squares	Polak-Ribière-Polyak (PRP) conjugate gradient	total variation (TV)	1.Introduce the concept of ICC 2.Use Fourier bases to represent noise gradient
	Discrete Exterior Calculus (DEC) method [23]	Pixel/voxel-based	3D	Least squares	Gauss-Newton method	multiplicative regularization (MR)	1.Provides a unified formulation for the discrete operators in different dimensions. 2.Compute efficiently, good reconstruction accuracy and anti-noise performance.
	Variational Space-Variant Model [48]	Pixel/voxel-based	2D	Variational	ADMM-Based Numerical Optimization	η-map	1.Introduce non-convex penalty to promote sparsity 2.Deal with the conductivity distributions of sharp and inhomogeneous variations
	size projection algorithm (SPA) [55]	Pixel/voxel-based	2D	Least squares	Golden-section search (GS) method	-	1.Propose the concept of projection error 2.The quantitative information of boundary is extracted by computing thresholding.
	Boolean operation [47]	Shape-based	2D	Least squares	Gauss-Newton method	Cholesky factorization	1.The sharp features were better preserved than STDFs-based approach. 2.Be tolerant to modeling errors caused by background inhomogeneity.
	Topological Derivative Method [71]	Shape-based	2D	Level set	Topological Derivative method	-	1. Ensure stability and greater accuracy of reconstruction results compared to an algorithm based solely on deterministic methods.
	Real-time Dynamic Imaging Method for Flexible Boundary Sensor in Wearable EIT [35]	Pixel/voxel-based	2D	- (linear model)	Back Projection (LBP)	regularization matrix	1. Consider the real-time changes of boundary in EIT. 2. Provides a quantitative method to describe boundary changes.
Stochastic method	Structure-Aware Sparse Bayesian Learning (SA-SBL) [34]	Pixel/voxel-based	2D	MAP estimation	SA-SBL algorithm	prior p(σ)	1. Exploit the structured sparsity in the conductivity distribution. 2. Achieve a higher spatial resolution.
	Multi-Task Structure-Aware Sparse Bayesian Learning (MT-SA-SBL) [33]	Pixel/voxel-based	2D	MAP estimation	MT-SA-SBL algorithm	prior p(σ)	1. Frequency-difference EIT is addressed in the MMV SBL framework for the first time. 2.Reduce the computational complexity compared with SA-SBL.
	Frequency Constrained Sparse Bayesian Learning (FC-SBL) [32]	Pixel/voxel-based	2D	MAP estimation	FC-SBL algorithm	prior p(σ)	1.Tackle the challenge of early diagnosis of acute stroke. 2.Strong regularizing and parameter-free properties.

3.2. Learning-Based Approach

An alternative approach for solving the EIT problem, which is always regarded as a regression problem, is deep learning (DL). Although DL has not yet had a wise impression on EIT as it has had for computer version field [40] that many researches have recently carried out. A brief review will be done in this section, and more detailed literatures on this topic can be found in [38–40].

Different from the model-based approach that uses the objective function to express the inverse mapping F^{-1} in Eq. (3) implicitly, the goal of learning-based method is to write an explicit expression of inverse mapping $\mathbf{F}^{-1}$ [38, 39] through the training stage, where the training strategy can be expressed as

$$\widehat{\theta} = \arg\min_{\theta} \sum_i f\left(\sigma_i, R_\theta\left\{\overline{V}_{n,i}\right\}\right) + g(\theta) \tag{12}$$

where R_θ is the neural network structure, and the parameter θ of the neural network framework can be learned by Eq. (12).

Once the parameters are determined, the inverse mapping $\mathbf{F}^{-1}$ can be expressed as R_θ parametrically. After the training (learning) stage, the result $\sigma(r)$ can be quickly predicted in the test stage.

Although DNN can potentially be used to approximate the inverse mapping $\mathbf{F}^{-1}$ due to its elasticity in representing high nonlinear functions as well as a data-driven regularization prior taken out automatically from the data [41], the direct learning approach actually works weakly if the input of the NN is set to the measured value, and the output is the value to be reconstructed as shown in Eq. (10). In that case, the tasks for DNN are very weighty; the accuracy of prediction is highly dependent on the training data, and only very simple impedance images are able to reconstruct [39]. In fact, in order to combine the good aspects of both approaches, researchers have used the amalgamation of model-based and learning-based approaches to solve the EIT problem. The emerging hybrid approach falls into two categories as follows:

Firstly, the scheme is still based on established model-based approach, but exerts NNs to learn a few components which are sometimes inflexible to deal with in the traditional framework. For example, CNNs, which have a strong learning capability and high representational capacity [38, 40], have been used to learn the noise-subspace components of contrast source in the subspace optimization method (SOM) [20]. In [56], the supervised descent method (SDM) is used to learn the sensitive matrix $\overline{\overline{\mathbf{J}}}$ as shown in Eq. (5). Compared with the traditional iterative method in model-based approach, SDM lessens the time and memory cost notably, and the priori knowledge is assimilated in a more pliable manner. Moreover, in [24], DL is used to optimize electrode positions for 2D EIT sensors.

Secondly, the physical knowledge and its mathematical realization are combined into the learning-based framework, where the input of neural network or the internal architecture of neural network is modified to avoid a black-box way. For example, in 2018, Dominant-Current Deep Learning Scheme (DC-DLS) inspired by BE-SOM [20] was proposed, where a well-suited U-net architecture was chosen and modified to solve EIT problems. The inputs are computed from induced contrast current (ICC), rather than the measured voltage, and the output is a single image of conductivity contribution. As a result, the reconstructed results by DC-DLS are capable of faster speed, higher quality of image and stability. Moreover, in 2019, a fully-convolutional neural network for electrical impedance maps (CNN-EIM) was presented [57], which brought the information of the symmetrical geometrical structure of tomographic sensors to learning-based image reconstruction. The results show that it can achieve higher quality for reconstruction and better generalization ability with a smaller number of learnable parameters than the direct learning approaches. Further, Wei and Chen [36] proposed an induced-current learning method (ICLM) to incorporate physical information into the deep learning method, which was inspired from nonlinear inverse scattering solvers [58, 59]. More specifically, ICLM learns a secondary source, i.e., induced contrast current (ICC), from the major part of ICC and the updated electrical field that are different with prevailing deep learning schemes.

3.3. Other Approaches

In the above, the EIT problem is described as a regression problem to reconstruct the conductivity distribution image. However, in some applications, a clear image is unnecessary, and it only requires to classify the reconstructional results. In 2020, Agnelli et al. proposed a machine learning method in EIT to classify stroke into either ischemic or hemorrhagic [25]. It is expected that in the future, there will be further researches of algorithm to be explored, and the application fields of EIT technology may be far more than what we see now.

4. HARDWARE IMPLEMENTS

Hardware system design is as fundamental as image reconstruction algorithm in EIT technology. More precisely, it plays a crucial role in exciting and contacting the object under test directly. Also, it is essential to both collecting and transmitting data. Due to the nonlinear and highly ill-posed property in inverse problem, the image reconstruction quality is very sensitive to the error measured by the physical instrument. Therefore, multifarious high-accuracy automatic measurement devices and advanced measurement methods have been proposed in recent decades to reduce the measurement noise

and inherent systematic errors. Meanwhile, the mode and speed of data transmission, convenience, power consumption, and cost are also the key indicators in medical imaging, where EIT system is always required to monitor the impedance changes of physiological and pathological states in real time.

This section will introduce the EIT system architecture and review the EIT systems built in recent years.

4.1. Electrode

Electrodes, located at the front end of the high-sensitivity detection system, contact human body directly. Any signals on the electrodes, including useful information, noise, artifact, contact impedance, polarization voltage, etc., will be amplified and processed in the subsequent circuit and affect the image reconstruction results finally [29]. Consequently, the design of electrode parameters is particularly important. The main principles to select suitable electrodes are summarized as follows:

- **Number.** Too few electrodes will reduce the measurement sensitivity, and too many electrodes will lessen the test speed. 16 electrodes are used in most systems.
- **Position.** It determines the amount of "high quality" information comprised in measurement processes, the conditioning of the EIT inverse problem, and the reliability of EIT measurements [24]. As a whole, the position of electrodes will influence the quality of reconstruction further.
- **Width.** For most EIT system, the excitation points and measurement areas are shared on the same electrodes. Therefore, the measuring "point" information may not be reflected by rule and line if the size is large, and excessive contact impedance would be lead if too narrow.
- **Material.** The conductivity of the electrode material must be much higher than that of the measured medium to ensure that the electrode surface is an equipotential surface.

Table 2. Four different types of excitation with superiority and inferiority.

Mode	adjacent mode	cross mode	oppsite mode	trigonometric mode
Expression	$I_i = \begin{cases} -j, & i = k \\ 0, & i \neq k, k + n \\ j, & i = k + n \end{cases}$			$I_i = jcos\left(\dfrac{2k}{N_r}i\right),$
	$n = 1$	$n = 3$	$n = \dfrac{N_r}{2}$	
$k = 1$				
$k = 2$				
Superiority	Well edge sensitivity	Balanced edge and overall sensitivity	Well overall sensitivity	Well edge, center, overall sensitivity and uniform current distribution
Inferiority	Poor center and overall sensitivity	Poor center sensitivity	Poor edge sensitivity	More independent current drivers and unknown contact impedance [17]

4.2. Excitation and Measurement

EIT is the inverse problem of determining the impedance in the interior of Ω, where it measures the ratio between the electric field and electric current. Spontaneously, there are two methods to obtain the electrical impedance. One method is to set stable voltage in the surface of object and then estimate the impedance distribution by the current obtained through the object. The mainstream method in EIT is to inject stable current into the object and estimate the impedance distribution by measuring the boundary voltage, which is discussed in this brief. In any case, we need excitation part and measurement part in EIT system.

• **Excitation mode.** We summarize four current injection modes [10, 17, 22, 60] in Table 2 with advantages and disadvantages, respectively.

• **Measurement mode.** The measurement strategies are usually divided into the two-electrode and four-electrode approaches. The current injection and voltage measurement are carried out from the same pair of electrodes in the former approach, where the strategy can be easily carried out, but the measurement values are always not accurate due to the contact impedance. As a comparison, four-electrode measurement strategy can effectively reduce the influence of contact impedance. More detailed researches on this topic can be found in [61, 62].

4.3. System Structure

According to different application fields, EIT systems have a single-source or multiple-source architecture. The former can present the advantage of less hardware, which means small size, low power consumption and cost, while the latter has fewer effects of stray capacitance [27] since it does not require multiplexers to switch channels of source and also reduces measurement time as measurements can be done in parallel.

Regardless of the difference, the basic block of an EIT system can be illustrated by Fig. 2. In brief, an embedded controller (i.e., FPGA) is needed to control the current source to produce steady current injected into object under test and A/D to sample the boundary voltage, and to send the data to a remote computing device (i.e., personal computer) for imaging reconstruction. In addition, some peripheral circuits need to be designed specially to adapt to different application fields. For example, in the medical imaging field, the amplitude of current source (i.e., VCCS) is less than $\pm 5\,\mathrm{mA}$ (the safety current of human body), and the center frequency is near low frequency (even a DC source, obtaining conductance information only). Correspondingly, the cut-off frequency of amplifier and filter is also needed to lay out reasonably.

Table 3. Some typical EIT systems in the recent decades.

System	OXBACT-5	KIT4	EIT Soc	EIT DAQ	Wireless EIT	Portable EIT	SWEIT	3D EIT
Publication	[64]	[66]	[4]	[65]	[68]	[67]	[63]	[18]
Year	2008	2008	2014	2015	2016	2018	2019	2020
Geometry	2D/3D	2D/3D	2D	2D	2D	2D	2D	2D/3D
Number of Electrodes	64	80	32	16	16	8	16	16
Source	Multiple	Multiple	Single	Single	Single	Single	Single	Single
Wearable	$\times$	$\times$	$\checkmark$	$\times$	$\checkmark$	$\times$	$\times$	$\checkmark$
Controller	FPGA	NI PXI-8916	ASICs	NI CompactRIO-9024	TI MSP430	Red Pitaya STEMlab	FPGA	FPGA
Frequency Range	1 kHz to 100 kHz	1 kHz–120 kHz	10, 50, 100, 200 Hz	DC	10 kHz to 200 kHz	0–100 kHz	1 kHz to 1.1 MHz (support chirp)	Set at 125 kHz
Interface	WLAN	PXI-bus	USB-OTG	10/100 base-t Ethernet LAN	Bluetooth v2.0 + EDR	LAN/SCPI	PCI-bus	UART
Resolution of ADC	14 bit	14 bit	-	24 bit	12 bit	-	-	12 bit
Major application	Distress and chronic heart failure (CHF)	Laboratory	Real-time lung ventilation monitoring	near-real-time spatial sensing	Human thorax image	Biomedical applications	Bioimpedance spectrum (BIS)	Hand Gesture Recognition
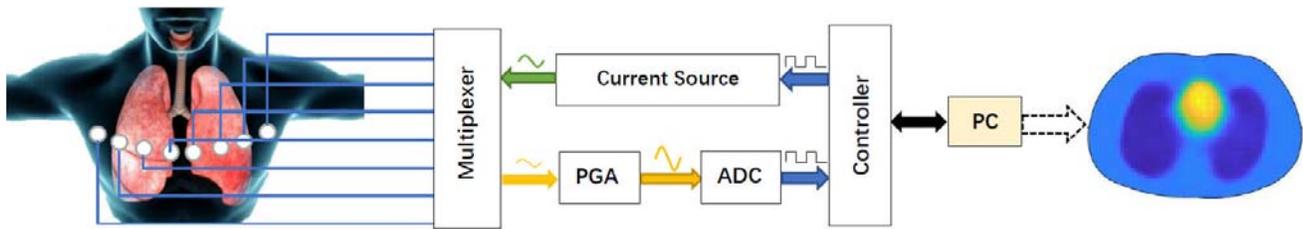
Figure 2. General block diagram of an EIT system.

Numerous EIT hardware systems have been applied in various fields or laboratories, and more detailed information about EIT hardware could be found in the monograph by Rymarczyk [69]. We summarize the characteristics of some typical EIT systems proposed recently in Table 3, where it can be seen that EIT system has the trend of light weight, wearability, and low power consumption.

5. CONCLUSIONS

This paper reviews the innovation and improvement of EIT technology in algorithms and hardware designs in recent years.

• **Algorithm.** Since EIT was proposed, the model-based approaches have been studied. Their implementation highly depends on a certain optimization criterion and needs to use certain prior knowledge for regularization. Usually, the reconstruction quality of non-iterative algorithm is poor, while the iterative algorithm has a large cost of calculation. With the development of deep learning methods, researchers have considered to apply the deep learning method in EIT image reconstruction algorithms, transferring the computational burden to the learning stage. Once the neural network is well trained, they can quickly and effectively generate accurate prediction. However, the learning method based on black-box is not ideal for EIT problems. One idea is to use deep learning to solve some highly nonlinear components under the framework of the model-based approach, which is always hard to deal with in traditional methods. The other one is to design the input, output, and neural network architecture to reduce the learning difficulty by utilizing some conclusions or techniques in model-based approaches. Therefore, future researches in algorithms may focus more on how to combine the advantages of both approaches to improve the quality of reconstruction. Further, different from model-based approaches, the reliability of learning approaches is limited. Thus, the uncertainty quantification [72] of the deep learning method in inversion will also be a future direction.

• **Hardware.** EIT equipments have tended to have higher precision, faster speed, more wearability, and lower power consumptio. At the same time, more and more design details have been considered by researchers, such as the influence of electrodes and excitation-measurement modes. For different application areas, the structures of EIT hardware may be different.

In the future, besides biomedical imaging and industry non-destructive fields, it is expected that EIT technology will find its applications in more fields, such as human-machine interaction.

REFERENCES

1. Williams, R. A. and M. S. Beck, "Chapter 1 — Introduction to process tomography," *Process Tomography*, Vol. 13, No. 2, 3–12, 1995.
2. Yang, L., C. Zhang, W. Liu, H. Wang, J. Xia, B. Liu, X. Shi, X. Dong, F. Fu, M. Dai, and J. L. Campos, "Real-time detection of hemothorax and monitoring its progression in a piglet model by electrical impedance tomography: A feasibility study," *BioMed Research International*, Vol. 2020, Article ID 1357160, 2020.
3. Schullcke, B., B. Gong, S. Krueger-Ziolek, et al., "Structural-functional lung imaging using a combined CT-EIT and a discrete cosine transformation reconstruction method," *Scientific Reports*, Vol. 6, 25951, 2016.

4. Hong, S., J. Lee, J. Bae, et al., "A 10.4 mW electrical impedance tomography SoC for portable real-time lung ventilation monitoring system," *IEEE Journal of Solid-State Circuits*, Vol. 50, No. 11, 2501–2512, 2015.

5. Boverman, G., T. J. Kao, X. Wang, et al., "Detection of small bleeds in the brain with electrical impedance tomography," *Physiol. Meas.*, Vol. 37, No. 6, 727–750, 2016.

6. Murphy, E. K., A. Mahara, and R. J. Halter, "Absolute reconstructions using rotational electrical impedance tomography for breast cancer imaging," *IEEE Transactions on Medical Imaging*, Vol. 36, No. 4, 892–903, 2017.

7. Sarode, V., S. S. Patkar, and A. N. Cheeran, "Comparison of factors affecting the detection of small impurities in breast cancer using EIT," *International Journal of Engineering Science & Technology*, Vol. 5, No. 6, 1267–1271, 2013.

8. Podczeck, F., C. L. Mitchell, J. M. Newton, et al., "The gastric emptying of food as measured by gamma-scintigraphy and electrical impedance tomography (EIT) and its influence on the gastric emptying of tablets of different dimensions," *Journal of Pharmacy & Pharmacology*, Vol. 59, No. 11, 1527–1536, 2010.

9. Tomasino, S., R. Sassanelli, C. Marescalco, et al., "Electrical impedance tomography and prone position during ventilation in COVID-19 Pneumonia: Case reports and a brief literature review," *Semin. Cardiothorac. Vasc. Anesth.*, Vol. 24, No. 4, 287–292, 2020.

10. Dickin, F. and M. Wang, "Electrical resistance tomography for process applications," *Measurement Science and Technology*, Vol. 7, No. 3, 247, 1996.

11. Tapp, H. S., A. J. Peyton, E. K. Kemsley, et al., "Chemical engineering applications of electrical process tomography," *Sensors & Actuators B: Chemical*, Vol. 92, No. 1/2, 17–24, 2003.

12. Kruger, M. V. P., "Tomography as a metrology technique for semiconductor manufacturing," PhD Thesis, University of California, Berkeley, 2003.

13. Linderholm, P., L. Marescot, M. H. Loke, et al., "Cell culture imaging using microimpedance tomography," *IEEE Transactions on Biomedical Engineering*, Vol. 55, No. 1, 138, 2008.

14. Sun, T., S. Tsuda, K. P. Zauner, et al., "On-chip electrical impedance tomography for imaging biological cells," *Biosensors & Bioelectronics*, Vol. 25, No. 5, 1109–1115, 2010.

15. Hou, T. C., K. J. Loh, and J. P. Lynch, "Electrical impedance tomography of carbon nanotube composite materials," *Proceedings of SPIE — The International Society for Optical Engineering*, 2007.

16. Hou, T. C., K. J. Loh, and J. P. Lynch, "Spatial conductivity mapping of carbon nanotube composite thin films by electrical impedance tomography for sensing applications," *Nanotechnology*, Vol. 18, No. 31, 962–969, 2007.

17. Liu, K., Y. Wu, S. Wang, et al., "Artificial sensitive skin for robotics based on electrical impedance tomography," *Advanced Intelligent Systems*, 1–13, 2020.

18. Jiang, D., Y. Wu, and A. Demosthenous, "Hand gesture recognition using three-dimensional electrical impedance tomography," *IEEE Transactions on Circuits and Systems II: Express Briefs*, Vol. 67, No. 9, 1554–1558, 2020.

19. Wang, Z., S. Yue, H. Wang, et al., "Data preprocessing methods for electrical impedance tomography: A review," *Physiological Measurement*, Vol. 41, No. 9, 09TR02, 2020.

20. Wei, Z., D. Liu, and X. Chen, "Dominant-current deep learning scheme for electrical impedance tomography," *IEEE Transactions on Biomedical Engineering*, Vol. 66, No. 9, 2546–2555, 2019.

21. Liu, D., V. Kolehmainen, et al., "Nonlinear difference imaging approach to three-dimensional electrical impedance tomography in the presence of geometric modeling errors," *IEEE Transactions on Biomedical Engineering*, Vol. 63, No. 9, 1956–1965, 2016.

22. Chitturi, V. and F. Nagi, "Spatial resolution in electrical impedance tomography: A topical review," *Journal of Electrical Bioimpedance*, Vol. 8, No. 1, 66, 2017.

23. Zhang, K., M. Li, et al., "Three-dimensional electrical impedance tomography with multiplicative regularization," *IEEE Transactions on Biomedical Engineering*, Vol. 13, No. 6, 1139–1159, 2019.

24. Smyl, D. and D. Liu, "Optimizing electrode positions in 2D Electrical Impedance Tomography using deep learning," *IEEE Transactions on Instrumentation and Measurement*, 2020.

25. Agnelli, J. P., A. Çöl, M. Lassas, et al., "Classification of stroke using neural networks in electrical impedance tomography," *Inverse Problems*, Vol. 36, No. 11, 115008, 2020.

26. Borcea, L., "Topical review: Electrical impedance tomography," *Inverse Problems*, Vol. 18, No. 6, R99, 2002.

27. Padilha Leitzke, J. and H. Zangl, "A review on electrical impedance tomography spectroscopy," *Sensors*, Vol. 20, No. 18, 2020.

28. Schwan, H. P., "Electrical properties of tissues and cell suspensions: Mechanisms and models," *International Conference of the IEEE Engineering in Medicine & Biology Society*, IEEE, 1994.

29. Somersalo, E., M. Cheney, and D. Isaacson, "Existence and uniqueness for electrode models for electric current computed tomography," *SIAM Journal on Applied Mathematics*, Vol. 52, No. 4, 1023–1040, 1992.

30. Jackson, J., *Classical Electrodynamics*, 3rd Edition, Wiley, 1998.

31. Cheng, K. S. and D. Isaacson, "Electrode models for electric current computed tomography," *IEEE Transactions on Biomedical Engineering*, Vol. 36, No. 9, 918–924, 1989.

32. Xiang, J., Y. Dong, and Y. Yang, "Multi-frequency electromagnetic tomography for acute stroke detection using frequency constrained sparse bayesian learning," *IEEE Transactions on Medical Imaging*, Vol. 39, No. 12, 4102–4112, 2020.

33. Liu, S., Y. Huang, H. Wu, et al., "Efficient multi-task structure-aware sparse bayesian learning for frequency-difference electrical impedance tomography," *IEEE Transactions on Industrial Informatics*, Vol. 17, No. 1, 463–472, 2021.

34. Liu, S., J. Jia, Y. D. Zhang, et al., "Image reconstruction in electrical impedance tomography based on structure-aware sparse Bayesian learning," *IEEE Transactions on Medical Imaging*, Vol. 37, No. 9, 2090–2102, 2018.

35. Darma, P. N., M. R. Baidillah, M. W. Sifuna, et al., "Real-time dynamic imaging method for flexible boundary sensor in wearable electrical impedance tomography," *IEEE Sensors Journal*, Vol. 20, No. 16, 9469–9479, 2020.

36. Wei, Z. and X. Chen, "Induced-current learning method for nonlinear reconstructions in electrical impedance tomography," *IEEE Transactions on Medical Imaging*, Vol. 39, No. 5, 1326–1334, 2019.

37. Wei, Z., R. Chen, H. Zhao, and X. Chen, "Two FFT subspace-based optimization methods for electrical impedance tomography," *Progress In Electromagnetics Research*, Vol. 157, 111–120, 2016.

38. Lucas, A., M. Iliadis, R. Molina, et al., "Using deep neural networks for inverse problems in imaging: Beyond analytical methods," *IEEE Signal Processing Magazine*, Vol. 35, No. 1, 20–36, 2018.

39. Chen, X., Z. Wei, M. Li, and P. Rocca, "A review of deep learning approaches for inverse scattering problems (invited review)," *Progress In Electromagnetics Research*, Vol. 167, 67–81, 2020.

40. Mccann, M. T., K. H. Jin, and M. Unser, "Convolutional neural networks for inverse problems in imaging: A review," *IEEE Signal Processing Magazine*, Vol. 34, No. 6, 85–95, 2017.

41. Fan, Y. and L. Ying, "Solving electrical impedance tomography with deep learning," *Journal of Computational Physics*, Vol. 404, 109119, 2019.

42. Xia, Z., Z. Cui, Y. Chen, et al., "Generative adversarial networks for dual-modality electrical tomography in multi-phase flow measurement," *Measurement*, 2020.

43. Kosowski, G. and T. Rymarczyk, "Using neural networks and deep learning algorithms in electrical impedance tomography," *Informatyka Automatyka Pomiary w Gospodarce i Ochronie Środowiska*, Vol. 7, No. 3, 99–102, 2017.

44. Hamilton, S. J. and A. Hauptmann, "Deep D-bar: Real time electrical impedance tomography imaging with deep neural networks," *IEEE Transactions on Medical Imaging*, Vol. 37, No. 10, 2367–2377, 2017.

45. Ren, S., K. Sun, C. Tan, et al., "A two-stage deep learning method for robust shape reconstruction with electrical impedance tomography," *IEEE Transactions on Instrumentation and Measurement*, Vol. 69, No. 7, 4887–4897, 2019.

46. Khan, T. A. and S. H. Ling, "Review on electrical impedance tomography: Artificial intelligence methods and its applications," *Algorithms*, Vol. 12, No. 5, 88, 2019.

47. Liu, D., D. Gu, D. Smyl, et al., "Shape reconstruction using boolean operations in electrical impedance tomography," *IEEE Transactions on Medical Imaging*, Vol. 39, No. 9, 2954–2964, 2020.

48. Huska, M., D. Lazzaro, S. Morigi, et al., "Spatially-adaptive variational reconstructions for linear inverse electrical impedance tomography," *Journal of Scientific Computing*, Vol. 84, No. 3, 2020.

49. Hamilton, S. J., J. L. Mueller, and T. R. Santos, "Robust computation in 2D absolute EIT (a-EIT) using D-bar methods with the 'exp' approximation," *Physiological Measurement*, Vol. 39, No. 6, 064005, 2018.

50. Chaulet, N., S. Arridge, T. Betcke, et al., "The factorization method for three dimensional electrical impedance tomography," *Mathematics*, Vol. 30, No. 4, 45005–45019(15), 2014.

51. Vauhkonen, M. and D. Vadasz, "Tikhonov regularization and prior information in electrical impedance tomography," *IEEE Transactions on Medical Imaging*, Vol. 17, No. 2, 285–293, 1998.

52. González, G., J. M. J. Huttunen, V. Kolehmainen, et al., "Experimental evaluation of 3D electrical impedance tomography with total variation prior," *Inverse Problems in Science & Engineering*, Vol. 2015, 1–21, 2015.

53. Gehre, M., T. Kluth, A. Lipponen, et al., "Sparsity reconstruction in electrical impedance tomography: An experimental evaluation," *Journal of Computational and Applied Mathematics*, Vol. 236, No. 8, 2126–2136, 2012.

54. Cherkaev, A. V. and L. V. Gibiansky, "Variational principles for complex conductivity, viscoelasticity, and similar problems in media with complex moduli," *Journal of Mathematical Physics*, Vol. 35, No. 1, 127–145, 1994.

55. Li, K., N. Yang, J. Wang, et al., "Size projection algorithm: Optimal thresholding value selection for image segmentation of electrical impedance tomography," *Mathematical Problems in Engineering*, Vol. 2019, No. 6, 1–11, 2019.

56. Li, M., K. Zhang, R. Guo, F. Yang, S. Xu, and A. Abubakar, "Supervised descent method for electrical impedance tomography," *2019 Photonics & Electromagnetics Research Symposium — Fall (PIERS — Fall)*, 2342–2348, Xiamen, China, December 17–20, 2019.

57. Hu, D., K. Lu, and Y. Yang, "Image reconstruction for electrical impedance tomography based on spatial invariant feature maps and convolutional neural network," *2019 IEEE International Conference on Imaging Systems and Techniques (IST)*, IEEE, 2019.

58. Wei, Z. and X. Chen, "Deep-learning schemes for full-wave nonlinear inverse scattering problems," *IEEE Transactions on Geoscience and Remote Sensing*, Vol. 57, No. 4, 1849–1860, 2018.

59. Wei, Z. and X. Chen, "Physics-inspired convolutional neural network for solving full-wave inverse scattering problems," *IEEE Transactions on Antennas and Propagation*, Vol. 67, No. 9, 6138–6148, 2019.

60. Bera, T. K. and J. Nagaraju, "Studying the resistivity imaging of chicken tissue phantoms with different current patterns in Electrical Impedance Tomography (EIT)," *Measurement*, Vol. 45, No. 4, 663–682, 2012.

61. Jones, D. M., R. H. Smallwood, D. R. Hose, et al., "Constraints on tetrapolar tissue impedance measurements," *Electronics Letters*, Vol. 37, No. 25, 1515–1517, 2002.

62. Chandra, H., S. W. Allen, S. W. Oberloier, et al., "Open-source automated mapping four-point probe," *Materials*, Vol. 10, No. 2, 110, 2017.

63. Tan, C., S. Liu, J. Jia, et al., "A wideband electrical impedance tomography system based on sensitive bioimpedance spectrum bandwidth," *IEEE Transactions on Instrumentation and Measurement*, Vol. 2019, 1–11, 2019.

64. Yue, X. and C. Mcleod, "FPGA design and implementation for EIT data acquisition," *Physiological Measurement*, Vol. 29, No. 10, 1233–1233, 2008.

65. Huang, S. K. and K. J. Loh, "Development of a portable electrical impedance tomography data acquisition system for near-real-time spatial sensing," *SPIE Proceedings*, Vol. 9435, 11 pages, 2015.

66. Kourunen, J., T. Savolainen, A. Lehikoinen, et al., "Suitability of a PXI platform for an electrical impedance tomography system," *Measurement Science & Technology*, Vol. 20, No. 1, 015503, 2012.

67. Xu, Z., J. Yao, Z. Wang, et al., "Development of a portable electrical impedance tomography system for biomedical applications," *IEEE Sensors Journal*, Vol. 18, 8117–8124, 2018.

68. Huang, J. J., Y. H. Hung, J. J. Wang, et al., "Design of wearable and wireless electrical impedance tomography system," *Measurement*, Vol. 78, 9–17, 2016.

69. Rymarczyk, T., *Tomographic Imaging in Environmental, Industrial and Medical Applications: Tomography, Internet of Things, Machine Learning, Distributed Systems, Big Data, Industry 4.0*, Innovation Press Publishing House, University of Economics and Innovation, 2019.

70. Rymarczyk, T., S. Filipowicz, and J. Sikora, "Comparing methods of image reconstruction in electrical impedance tomography," *Computer Applications in Electrical Engineering*, 2011.

71. Rymarczyk, T., "Minimization of objective function in electrical impedance tomography by topological derivative," *Przeglad Elektrotechniczny*, Vol. 1, No. 6, 139–142, 2019.

72. Wei, Z. and X. Chen, "Uncertainty quantification in inverse scattering problems with bayesian convolutional neural networks," *IEEE Transactions on Antennas and Propagation*, IEEE, 2020.